Maternal Torso-Like Coordinates Tissue Folding During *Drosophila* Gastrulation

Travis K. Johnson,*,†,1 Karyn A. Moore,* James C. Whisstock,†,‡,1,2 and Coral G. Warr*,†,1,2
*School of Biological Sciences, †Australian Research Council Centre of Excellence in Advanced Molecular Imaging, and ‡Department of Biochemistry and Molecular Biology, Monash University, Clayton, Victoria 3800, Australia

ABSTRACT The rapid and orderly folding of epithelial tissue during developmental processes such as gastrulation requires the precise coordination of changes in cell shape. Here, we report that the perforin-like protein Torso-like (Tsl), the key extracellular determinant for *Drosophila* embryonic terminal patterning, also functions to control epithelial morphogenesis. We find that *tsl* null mutants display a ventral cuticular hole phenotype that is independent of the loss of terminal structures, and arises as a consequence of mesoderm invagination defects. We show that the holes are caused by uncoordinated constriction of ventral cell apices, resulting in the formation of an incomplete ventral furrow. Consistent with these data, we find that loss of *tsl* is sensitive to gene dosage of *RhoGEF2*, a critical mediator of Rho1-dependent ventral cell shape changes during furrow formation, suggesting that Tsl may act in this pathway. In addition, loss of *tsl* strongly suppressed the effects of ectopic expression of Folded Gastrulation (Fog), a secreted protein that promotes apical constriction. Taken together, our data suggest that Tsl controls Rho1-mediated apical constriction via Fog. Therefore, we propose that Tsl regulates extracellular Fog activity to synchronize cell shape changes and coordinate ventral morphogenesis in *Drosophila*. Identifying the Tsl-mediated event that is common to both terminal patterning and morphogenesis will be valuable for our understanding of the extracellular control of developmental signaling by perforin-like proteins.

KEYWORDS morphogenesis; gastrulation; Torso-like; MACPF; *Drosophila*

MORPHOGENESIS is the fundamental biological process by which organisms acquire their form, and involves a complex orchestration of cell fate decisions and gross movements of cell populations. The cell movements that occur during morphogenesis are governed by concerted tissue-wide changes to cellular shape (Ip and Gridley 2002; Sawyer *et al.* 2010). One of the best studied examples of morphogenesis is the early stages of gastrulation in the *Drosophila* embryo, whereby cells in defined regions of the embryo are rapidly internalized (Leptin and Grunewald 1990; Knust and Muller 1998). The two major morphogenetic movements that occur during *Drosophila* gastrulation are the invaginations of the ventral furrow and the posterior midgut (Leptin and Grunewald 1990; Sweeton *et al.* 1991; Leptin *et al.* 1992). These events occur 3-hr postfertilization, immediately following the completion of cellularization, and serve to bring mesodermal and endodermal precursors to the interior of the embryo (Wieschaus and Nüsslein-Volhard 1986; Leptin 1995).

Underpinning these tissue invaginations is the ability of cells to constrict at their apical edges and adopt a wedge-like shape [for review see Lecuit and Lenne (2007)]. Intracellularly, this occurs via the remodelling of the actomyosin cytoskeleton, while cytoskeleton-linked connections between neighboring cells known as adherens junctions (AJs) provide tensile strength to allow the tissue to fold as a sheet (Martin *et al.* 2010). A remarkable aspect of *Drosophila* ventral morphogenesis is the rapid speed at which it occurs (Kam *et al.* 1991; Oda and Tsukita 2001). It is therefore critical that the apical constriction of individual ventral cells is precisely timed and synchronized across the entire ventral domain to permit a productive furrow that can complete invagination.

The key developmental signal that is required to initiate apical constriction is encoded by Folded Gastrulation (Fog) (Costa *et al.* 1994). Fog is a secreted protein that becomes expressed in subsets of cells fated for actomyosin-based shape changes, for example in the ventral mesoderm prior

doi: https://doi.org/10.1534/genetics.117.200576
Manuscript received January 25, 2017; accepted for publication May 4, 2017; published Early Online May 9, 2017.
Supplemental material is available online at www.genetics.org/lookup/suppl/doi:10.1534/genetics.117.200576/-/DC1.
[1]Corresponding authors: Monash University, Wellington Road, Clayton, VIC 3800, Australia. E-mails: coral.warr@monash.edu; travis.johnson@monash.edu; and james.whisstock@monash.edu
[2]These authors contributed equally to this work and are joint senior authors.

to ventral furrow formation (Costa *et al.* 1994). Fog is thought to signal to a local field of cells via the G-protein-coupled receptor Mesoderm-invagination signal transducer (Mist) Manning *et al.* 2013). Upon binding of Fog, localized activation of Mist induces apical constriction in cells of the presumptive mesoderm via G-protein signaling and activation of the highly conserved GTPase Rho1 by its guanine nucleotide exchange factor RhoGEF2 (Barrett *et al.* 1997; Morize *et al.* 1998; Nikolaidou and Barrett 2004; Dawes-Hoang *et al.* 2005; Manning *et al.* 2013). Rho1 activates Rho kinase, which phosphorylates the regulatory light chain of nonmuscle myosin II to induce contraction of the apical actomyosin network in the cells that receive the Fog signal (Dawes-Hoang *et al.* 2005).

As well as promoting apical constriction, the Fog/Mist pathway has been implicated as a central regulator of its coordination between cells. In addition to delayed initiation of morphogenesis, *fog* mutants display uncoordinated ventral cell apical constriction, a highly disorganized ventral furrow, and often fail to complete invagination (Costa *et al.* 1994; Oda and Tsukita 2001). However, unlike its role in initiating constriction, the mechanism by which the Fog pathway coordinates constriction between cells remains to be elucidated.

Here, we report that the maternal patterning protein Torso-like (Tsl), long known as the localized determinant of embryonic terminal patterning (Stevens *et al.* 1990; Savant-Bhonsale and Montell 1993; Martin *et al.* 1994), is also essential for the promotion and coordination of mesoderm invagination. Our data implicate Tsl as a new extracellular member of the Fog/Mist pathway required for ventral morphogenesis in *Drosophila*, and suggest that, while terminal patterning and ventral morphogenesis are distinct in many ways, these processes may share a common regulatory mechanism.

Materials and Methods

Drosophila stocks and maintenance

The following stocks were used: w^{1118} (BL5905), tsl^{Δ} (Johnson *et al.* 2013), tor^{XR1} (Sprenger *et al.* 1989), *HA-Tsl* (Jimenez *et al.* 2002), tsl^{2}, tsl^{3}, tsl^{4}, tsl^{5} (Savant-Bhonsale and Montell 1993), *slbo*-Gal4 (Rorth *et al.* 1998), *Ecad-GFP* (Oda and Tsukita 2001), fog^{S4} (BL2100), $RhoGEF2^{4.4}$ (BL9382; Barrett *et al.* 1997), and *Gal4*::*VP16-nos.UTR* (BL7253). All flies were maintained on standard media at 25°.

Cloning and transgenesis

To generate the upstream activating sequence (UAS)-*Tsl-GFP* construct, the open reading frame of *tsl* followed by a short linker encoding the peptide SAGSAS, three tandem myc epitopes, and the open reading frame for enhanced GFP (eGFP) was synthesized (Genscript) and subcloned in pUASTattB via *Bgl*II and *Xho*I sites. For UASP-*fog*, the full-length *fog* cDNA transcript was excised from an existing clone (SD02223; Rubin *et al.* 2000) and inserted into pUASP (Rorth 1998) via *Eco*RI/*Xho*I. Transgenic lines were made (BestGene) via ΦC31integrase-mediated transformation (Bischof *et al.* 2007) using the ZH-51CE attP-landing site for UAS-*Tsl-GFP*, and standard *P*-element transformation methods (Rubin and Spradling 1982) for genomic integration of UASP-*fog* into the w^{1118} background.

Cuticle preparations

Adults were allowed to lay on media containing apple juice supplemented with yeast paste for 24 hr before being removed. Embryos developed for a further 24 hr before dechorionation in 50% (v/v) bleach and mounting on slides in a 1:1 (v/v) mixture of Hoyer's solution:lactic acid. Slides were incubated for several hours or overnight at 65° and imaged using dark-field optics (Leica). Cuticles from at least three separate overnight lays were scored and the means of each phenotypic category calculated. Significant differences between genotypes were determined by two-tailed unpaired *t*-tests.

Immunohistochemistry

For immunostaining, adults of the genotypes indicated were allowed to lay for 5 hr or overnight to isolate gastrulae and late-staged embryos, respectively. Embryos were collected, dechorionated, and either heat-fixed (for anti-β-cat) by pouring boiling salt solution (70 mM NaCl and 0.03% Triton X-100) over the embryos and cooling immediately on ice, or by chemical fixation (100 mM PIPES pH 6.9, 2 mM EGTA, 1 mM $MgSO_4$, and 4% formaldehyde) with an equal volume of n-heptane for 25 min rocking. Embryos were devitellinized with n-heptane and methanol and rehydrated with phosphate buffered saline (PBS) with 0.1% Triton X-100 (PTx) before being blocked for 1 hr in PTx containing 5% normal goat serum (Sigma [Sigma Chemical], St. Louis, MO). Primary antibodies (anti-Nrt, 1:50; anti-β-cat, 1:20; and anti-Twi, 1:1000) were diluted in fresh block solution and incubated overnight with shaking at 4°. Secondary antibodies (anti-mouse and rabbit Alexa488 and 588 conjugated, 1:500, Molecular Probes, Eugene, OR) were applied after several washes in PTx for 1 hr, washed further, stained with DAPI (Sigma), and mounted in vectashield (Vector Laboratories, Burlingame, CA). Embryos were left whole, or hand-sliced using a 21-gauge needle and imaged using a spinning disk confocal microscope (Olympus CV1000).

RNA in situ hybridizations

RNA *in situ* hybridizations on whole-mount, 4-hr-old fixed (4% paraformaldehyde in phosphate buffered saline), and methanol devitellinized embryos were performed using a DIG-labeled antisense RNA probe transcribed from a pGEMT-Easy (Promega, Madison, WI) clone of *sna* (F-5′-CGCAGGATCTATCCCTGAAA-3′, R-5′-AGCGACATCCTGGAGAAAGA-3′) following standard protocols (Tomancak *et al.* 2002). Briefly, probes were hybridized to embryos overnight at 55° and washed in hybridization buffer (4 × saline sodium citrate buffer, 50% v/v formamide, 0.1% v/v Tween-20, and 50 mg/ml heparin) for 36 hr before incubation with alkaline

phosphatase-conjugated anti-DIG and color development with 5-bromo-4-chloro-3-indolyl phosphate and nitro blue tetrazolium chloride. Imaging was performed under differential interference contrast optics on a Leica DM LB compound microscope.

Live imaging

Flies were allowed to lay for 4 hr and their embryos collected, dechorionated, and placed ventral side down in the wells of an eight-chambered slide and covered in PBS. Following the completion of cellularization, 10 optical slices, covering a 20 μm range starting at the ventral surface, were captured every 30 sec for each embryo using a 20 × objective (UPLSApo, 0.7NA) and CV1000 microscope. Movies were generated at 10 frames per second using images captured 9 μm below the embryo surface.

Data availability

Data and reagents are available upon request. Supplemental Material, File S1 contains one figure and the legends for File S2 and File S3.

Results

We previously generated a null mutant of *tsl* (tsl^{Δ}) via ends-out gene targeting (Johnson *et al.* 2013), as the available *tsl* alleles (*e.g.*, $tsl^{1\text{-}5}$ and tsl^{00617}; Stevens *et al.* 1990; Savant-Bhonsale and Montell 1993) were point mutations or *P*-element insertions and potentially hypomorphic. As expected, and similar to observations for other maternal terminal class genes, embryos laid by tsl^{Δ} homozygous females lacked terminal structures (including abdominal segment 8, the telson, and filzkorper, Figure 1, B and C). Strikingly however, a large proportion (> 90%) of these embryos also displayed ventrally-located cuticular holes (Figure 1, D and E). These holes were variable in size and number and most often occurred in the posterior region of the embryo (Figure S1 in File S1).

To ensure that this phenotype was due to loss of *tsl*, we first performed complementation tests with other available *tsl* alleles. Placing the tsl^{Δ} allele *in trans* with chromosomes carrying tsl^{2} or tsl^{3} alleles produced embryos with only terminal defects and no ventral holes (Figure 1E). However, in transheterozygotes for tsl^{Δ} and the tsl^{4} and tsl^{5} alleles, both of which are known to be stronger with respect to the terminal class phenotype (Savant-Bhonsale and Montell 1993), cuticular holes were readily observed (Figure 1E). We also performed a rescue experiment using a genomic *tsl* construct in which Tsl is tagged at the N-terminus by a hemaglutinin (HA) epitope (*HA-Tsl*; Jimenez *et al.* 2002). We have previously shown that this transgene fails to rescue the terminal patterning defects in tsl^{Δ} embryos (Johnson *et al.* 2013), possibly due to its inability to accumulate at the embryonic plasma membrane (Mineo *et al.* 2015). Despite this, *HA-Tsl* fully rescues the ventral hole phenotype (Figure 1F).

In terminal patterning, maternal Tsl originates from ovarian follicle cells at the anterior and posterior poles of the developing oocyte (Stevens *et al.* 1990; Savant-Bhonsale and Montell 1993; Martin *et al.* 1994). Given the maternal nature of both the terminal and the cuticular hole phenotypes, we were interested to know whether the latter phenotype is also caused by loss of *tsl* from the follicle cells, or whether it reflects an unreported expression pattern of *tsl*. To this end, we expressed a functional UAS transgene encoding a carboxy-terminal eGFP-tagged form of Tsl (*Tsl-eGFP*) in the *tsl* null background specifically in the ovarian follicle cells that are known to express *tsl* (using *Slbo*-Gal4; Rorth 1998). Strikingly, these embryos showed full restoration of the ventral cuticle (Figure 1, E and G). These data strongly suggest that the ventral cuticular hole phenotype is due to a loss of maternal *tsl* from the same cells in which it is needed for terminal patterning.

Having established that loss of *tsl* was the cause of the cuticular holes, we next wanted to pinpoint the origins of the defect during embryogenesis. Given the ventral location of the holes, we reasoned that *tsl* might function in an aspect of early ventral development such as patterning or morphogenesis. Therefore, we first asked whether ventral cell fate is specified correctly in tsl^{Δ} embryos by examining *snail* (*sna*) expression, a well-known marker for ventral cell differentiation (Leptin *et al.* 1992). To ensure that any deviations from wild-type that we observed were not due to the terminal class mutant phenotype, we compared tsl^{Δ} embryos to control terminal class mutant embryos that did not display the cuticular holes. For this, we used either *HA-Tsl*; $tsl^{\Delta}/tsl^{\Delta}$ embryos (as their genetic background is very close to that of tsl^{Δ}) or, when large numbers of embryos were required for precisely timed fixations, homozygotes of the *tor* null allele tor^{XR1} (Sprenger *et al.* 1989).

No obvious defects in the *sna* expression domain were seen in tsl^{Δ} embryos, with the exception of its extension posteriorly to the pole (a known consequence of lacking posterior Tor signaling), and also observed in the control terminal mutant embryos (Figure 2, A–C; Leptin and Grunewald 1990; Ray *et al.* 1991). These data suggest that the cuticular hole phenotype is unlikely to be due to a failure of ventral fate specification.

To determine whether morphogenesis is instead affected by loss of *tsl*, tsl^{Δ} embryos were stained for the membrane marker Neurotactin (Nrt), which becomes concentrated at the apical region of constricting cells (Hortsch *et al.* 1990). In contrast to wild-type embryos, which formed normal furrows (Figure 2D), and to terminal class mutant embryos, that formed a largely normal but extended furrow (Figure 2E), tsl^{Δ} embryos formed irregular and often incomplete ventral furrows (Figure 2F). Imaging the dorsal side of ~4.5-hr-old tsl^{Δ} embryos revealed defects in the extended germband. As expected for terminal class embryos, and also seen in the terminal class mutant control (Figure 2H), the posterior midgut invagination failed, leaving the pole cells at the dorsal surface rather than being internalized (Figure 2 compare G and H with I; Costa *et al.* 1994). By contrast, in tsl^{Δ} embryos an additional large field of cells posterior to the pole cells was

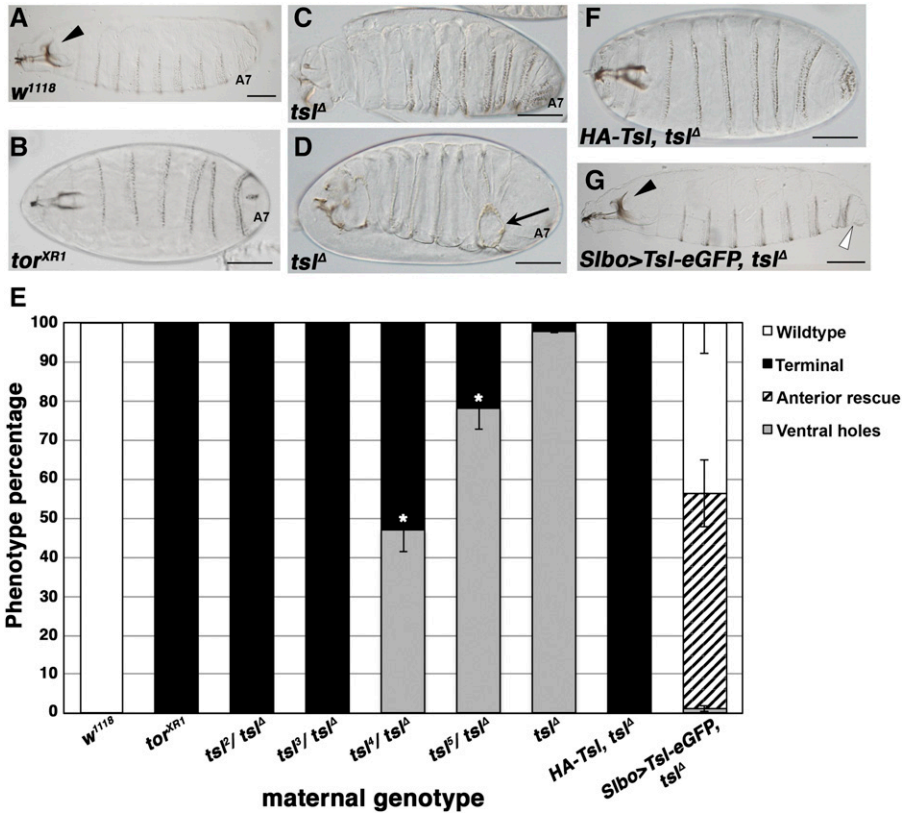

Figure 1 Loss of maternal *tsl* results in ventral cuticular holes that are independent of terminal patterning failure. (A) Wild-type larval cuticle with complete head skeleton (arrowhead) and abdominal segment 7 (A7) present. (B) Cuticle of embryos laid by tor^{XR1} females showing the terminal class mutant phenotype. Note that the head skeleton is reduced and structures posterior to A7 are absent. (C and D) Cuticles of embryos laid by tsl^{Δ} mothers display the terminal phenotype (C) similar to tor^{XR1}; however, a large proportion also possess ventral cuticular holes (D, arrow). (E) Quantification of phenotypes observed in embryos laid by mothers of the genotypes shown. Hypomorphic alleles of *tsl in trans* with the null allele (tsl^{Δ}) form an allelic series with respect to the cuticular hole phenotype. Asterisks indicate significant differences from the tsl^{Δ} phenotype (*t*-test, $P < 0.05$). Means are plotted and error bars represent one SE calculated from at least three cuticle preparations (> 100 cuticles scored for each). (F) A genomic transgene containing HA-tagged *tsl* (*HA-Tsl*) completely rescues the cuticular hole phenotype of tsl^{Δ}; however, it does not restore terminal patterning. (G) Expression of an enhanced GFP (eGFP)-tagged *tsl* transgene in the endogenous ovarian pattern of *tsl* (*Slbo*-Gal4) restores the tsl^{Δ} ventral cuticle and partially restores terminal patterning, as assessed by rescue of the anterior head skeleton and presence of abdominal segment 8. The cuticle shown is a representative image where the addition of A8 tissue (open arrowhead) and a wild-type head skeleton (arrowhead) is observed. Anteriors are to the left. Bar, 100 μm.

observed (Figure 2I). We reasoned that these cells might be mesodermal tissue remaining at the embryo surface as a consequence of invagination failure. To confirm this, we stained tsl^{Δ} embryos with anti-Twist (Twi), a marker of the presumptive mesoderm (Leptin and Grunewald 1990). Twi-positive cells were not detected at the surface of wild-type nor terminal class mutant embryos following ventral furrow invagination, indicating their successful internalization (Figure 2, J and K). However, in tsl^{Δ} embryos, Twi-positive cells were readily visible at the surface indicating regional invagination failure (Figure 2L). Collectively, these data strongly suggest that *tsl* functions to promote invagination of the ventral mesoderm during morphogenesis.

A failure of invagination is most commonly due to defects in apical constriction. Therefore, we assessed constriction at the onset of ventral furrow formation by staining embryos for β-catenin, an integral intracellular component of the AJ (Cox *et al.* 1996). In wild-type embryos, strong and uniform apical accumulation of β-catenin was observed in constricting ventral cells (Figure 3A). This was also observed in control terminal class mutant embryos that did not display the cuticular holes (Figure 3B). By contrast, in tsl^{Δ} embryos, ventral cells that were attempting furrow formation showed greatly reduced levels of apical β-catenin, often coinciding with incorrectly positioned nuclei close to the apical surface (Figure 3C). These cells were misaligned at their apical edges, suggesting apical constriction failure, and likely underlying the inconsistent and poorly formed early furrow. These defects were particularly evident at the posterior ends of tsl^{Δ} embryos (Figure 3, D–F), corresponding with the final position of the cuticular holes. Therefore, these data strongly suggest that the holes are caused by furrow defects.

Our observation that not all tsl^{Δ} embryos displayed defects in furrow formation suggested that *tsl* is important but not essential for apical constriction, and thus may perform a regulatory role in morphogenesis. Therefore, we hypothesized that *tsl* might be required to coordinate the timing of apical constriction across the ventral domain. To investigate this, we imaged ventral morphogenesis live in embryos expressing Ecad-GFP (Oda and Tsukita 2001), a marker of the AJ. Control (Ecad-GFP) embryos showed the characteristic rapid and coordinated apical constriction and internalization of a band of ventral cells following cellularization (Figure 3, G, I, and K and File S2). In contrast, in tsl^{Δ} embryos there was a delay in the initiation of ventral apical constriction of ~8 min. However, once constriction initiated in tsl^{Δ} embryos, the timing of tissue folding appeared relatively normal. We noted that the action of the furrow was wave-like rather than simultaneous, with the most constricted patches invaginating first, and appearing to pull less constricted cells into the furrow along with them. In agreement with the fixed embryo cross-sections, constriction was highly irregular and limited to seemingly random patches of cells across the ventral domain (Figure 3H and File S3). Furthermore, we commonly

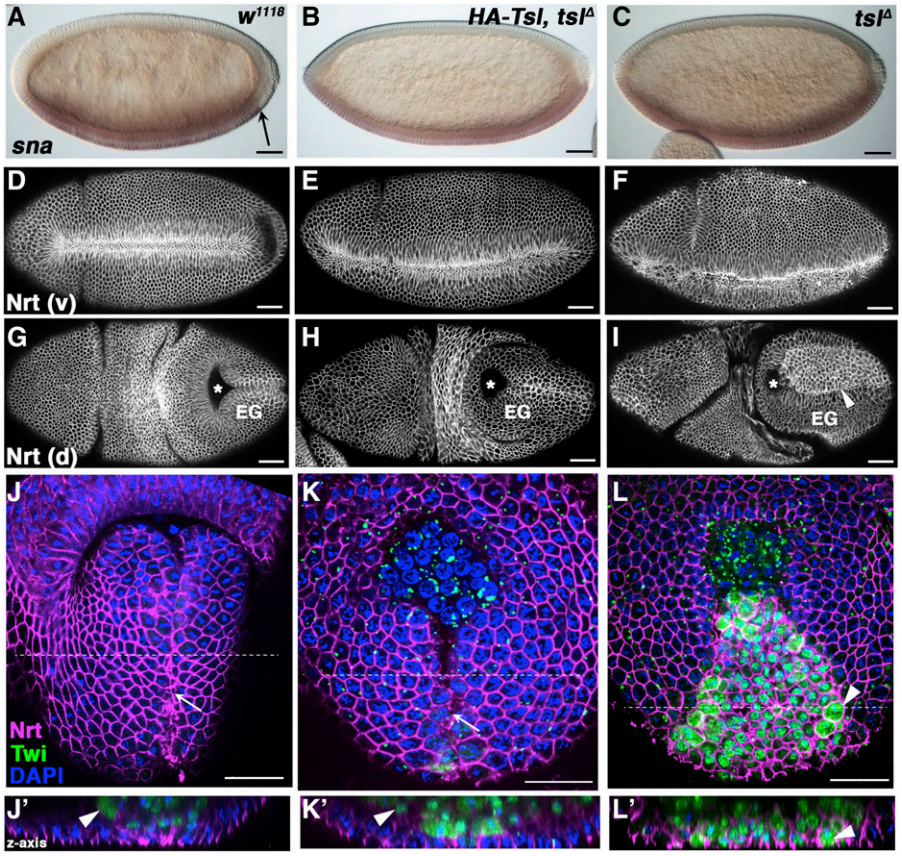

Figure 2 The ventral cuticular holes in *tsl*$^{\Delta}$ embryos are caused by impaired mesoderm invagination during morphogenesis. Wild-type (*w*^{1118}, left panels), terminal class mutant (*HA-Tsl*, *tsl*$^{\Delta}$, center panels), and *tsl*$^{\Delta}$ (right panels) embryos stained with various markers of embryogenesis. (A–C) Transcript expression of the ventral cell fate marker *Snail* (*sna*) is repressed at the posterior of wild-type embryos by the terminal system (A, arrow). In *tsl*$^{\Delta}$ (B) and terminal class mutant (C) embryos, *sna* expression extends to the posterior pole. (D–F) Ventral (v) furrow formation in gastrulating embryos labeled with the membrane marker anti-Neurotactin (Nrt). Wild-type (D) and terminal class mutant (E) embryos form regular ventral furrows. The furrows from *tsl*$^{\Delta}$ embryos are irregular and incomplete (F). (G–I) Dorsal (d) views of gastrulated embryos stained with anti-Nrt. (G) Wild-type embryos correctly invaginate their posterior midgut (pole cell position indicated by asterisks) unlike terminal class mutant (H) and *tsl*$^{\Delta}$ (I) embryos due to terminal system failure. however, *tsl*$^{\Delta}$ embryos possess a large field of intensely labeled cells on the extended germband (EG) that are not seen in wild-type nor terminal class mutant embryos (arrowhead). Anteriors are to the left. (J–L) Posterior–dorsal surface views of gastrulae embryos stained with anti-Nrt (magenta), anti-Twist (Twi, green) to label mesodermal precursors, and DAPI (blue). The ventral furrow has closed at the midline (white arrow) in wild-type (J) terminal class mutant (K) embryos but remains open in *tsl*$^{\Delta}$ embryos (L), as indicated by the surface location of Twi-positive cells (white arrowheads). Anteriors are to the top. Lower panels (J'–L') show the *z*-axis cross-section of the top panels at the position indicated by the dotted white line. Twi-positive nuclei are visible only below the dorsal surface in wild-type (J') and terminal class mutant (K') embryos indicating successful furrow invagination. Many of these cells remain at the dorsal surface of *tsl*$^{\Delta}$ embryos (L'). Maternal genotypes are shown. Bar, 50 μm.

observed apical constriction failure in a large proportion of posterior–ventral cells, often corresponding with a failure of the entire posterior half of the embryo mesoderm to invaginate (Figure 3L, compare to K). Taken together, these support the idea that Tsl both promotes and coordinates apical cell constriction during early furrow formation.

Cell shape changes that occur during *Drosophila* gastrulation require the activity of the Rho1 pathway (Barrett *et al.* 1997; Nikolaidou and Barrett 2004; Kolsch *et al.* 2007). Since loss of *tsl* causes defects in apical constriction, we next asked if Tsl might function in this pathway. To test this, we took advantage of the variation in the *tsl*$^{\Delta}$ cuticle phenotype and investigated whether reducing the gene dosage of *RhoGEF2*, which encodes the upstream activator of Rho1, could enhance its severity. Loss of either RhoGEF2 or Rho1 results in an identical phenotype whereby no ventral furrow forms (Barrett *et al.* 1997; Hacker and Perrimon 1998; Nikolaidou and Barrett 2004; Dawes-Hoang *et al.* 2005). We found that reducing *RhoGEF2* gene dosage (*RhoGEF2*$^{4.4}$/+) strikingly enhanced the severity of the *tsl*$^{\Delta}$ cuticular phenotype, resulting in all embryos missing their entire ventral cuticle (Figure 4, B and C). This finding suggests that Tsl activity during ventral morphogenesis requires the function of RhoGEF2.

In terminal patterning Tsl acts extracellularly and upstream of the Tor receptor ligand Trk (Casanova and Struhl 1989; Stevens *et al.* 1990; Sprenger and Nusslein-Volhard 1992). Recently, we have reported that Tsl likely achieves this by controlling the extracellular accumulation of Trk (Johnson *et al.* 2015). Therefore, we hypothesized that in gastrulation Tsl may regulate a receptor/ligand pathway upstream of the effectors RhoGEF2 and Rho1. The only extracellular molecule known to act upstream of Rho1 in *Drosophila* ventral morphogenesis is the zygotically-expressed protein Fog (Costa *et al.* 1994; Dawes-Hoang *et al.* 2005). Loss of Fog has been reported to result in ventral defects similar to the phenotypes observed here for *tsl*$^{\Delta}$, including uncoordinated ventral apical constriction (Costa *et al.* 1994; Oda and Tsukita 2001) and ventral cuticle holes (Wieschaus *et al.* 1984; Zusman and Wieschaus 1985). In addition, we noted that *fog* mutant (*fog*^{s4}/Y) cuticle holes were often positioned at the posterior (Figure 4D), as observed in embryos laid by *tsl*$^{\Delta}$ females (Figure 1D), further indicating that the two genes may be acting in the same pathway.

If Tsl acts in the Fog pathway then we might expect that the combination of loss of *fog* and loss of terminal patterning

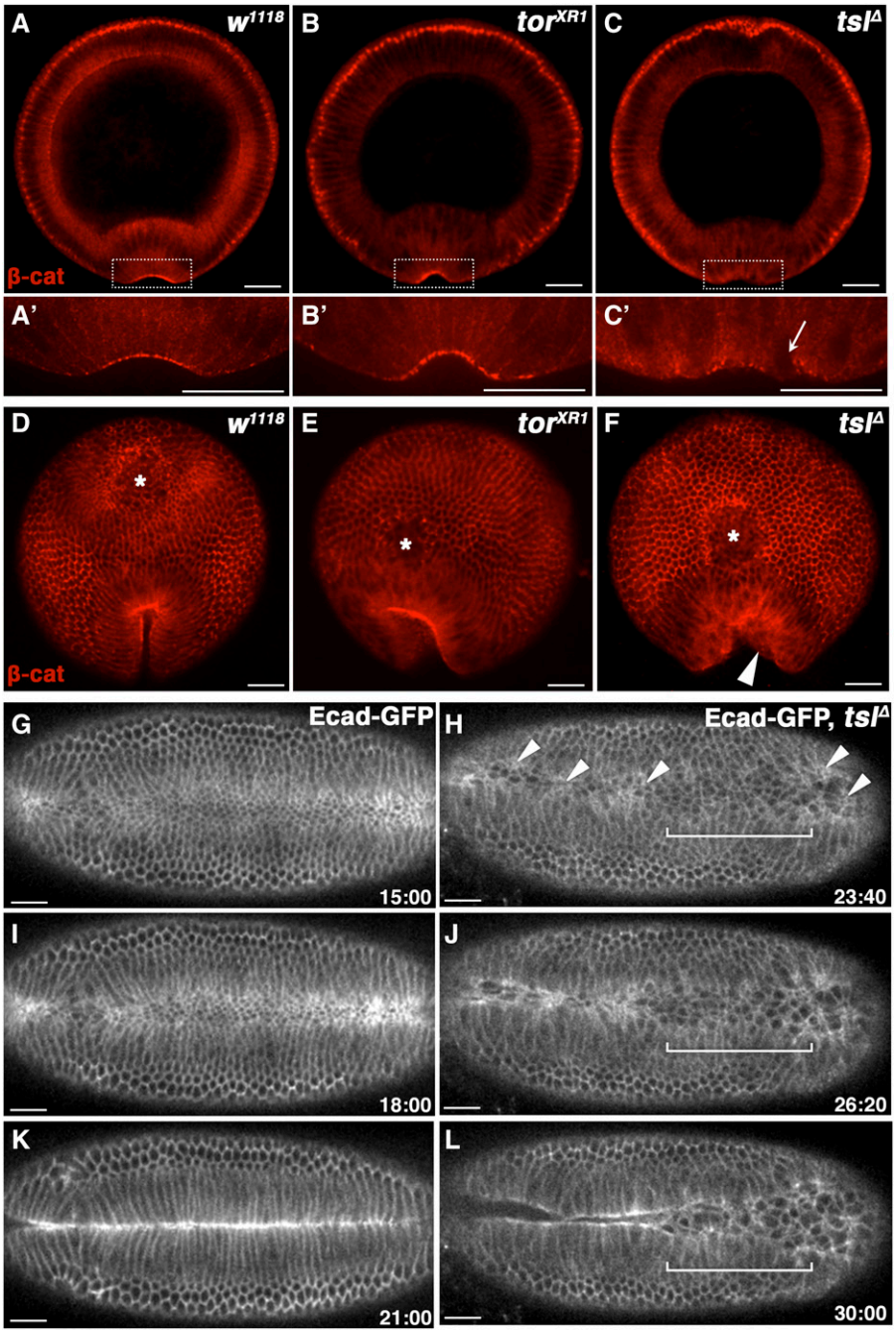

Figure 3 Tsl promotes and coordinates apical constriction during ventral furrow formation. (A–C) Cross-sections of fixed early gastrulae embryos sectioned at approximately two-thirds the embryo length (from the anterior to posterior) and labeled with anti-β-catenin to reveal adherens junctions (AJs). β-catenin localizes strongly to the apical surface in the early ventral furrow in wild-type (w^{1118}, A) and terminal class mutant (tor^{XR1}, B) embryos, but poorly and irregularly in tsl^{Δ} embryos (C). Lower panels are (A'–C') high-magnification images of the boxed area in the top panels. Areas of low apical β-catenin correspond to unconstricted cells indicated by apical nuclei (arrowed). Posterior view of embryos with closing ventral furrows. Uniform furrows and concentrated apical AJs are observed for wild-type (D) and terminal class mutant (E) embryos, despite the latter failing to internalize the posterior midgut (asterisks) and forming a posteriorly extended furrow as expected. tsl^{Δ} embryos fail similarly in these regards; however, they also display an irregular shaped posterior furrow (F, arrowhead). Ventral is to the bottom. (G–L) Live imaging stills taken at 3-min intervals of representative Ecad-GFP-expressing control (G, I, and K) and tsl^{Δ} (H, J, and L) embryos during ventral furrow formation and invagination. Furrow formation in tsl^{Δ} embryos is delayed by ~8 min compared to controls. Cell constrictions in the ventral domain of tsl^{Δ} embryos are limited to sporadic patches of cells (arrowheads). Areas containing more constricted cells appear to initiate furrow formation first. Invagination is incomplete in this example due to a large population of cells toward the posterior (bracketed) remaining unconstricted. Time is in minutes postcellularization completion. Ventral side is shown with anteriors to the left. Maternal genotypes are indicated. Bar, 35 μm.

would replicate the overall phenotype of tsl^{Δ}. Consistent with this idea, we found that embryos mutant for *fog* while also lacking the maternal contribution of *tor* produced cuticles that closely resemble the tsl^{Δ} cuticle (Figure 4E). To more directly determine whether Fog activity requires Tsl, we ectopically expressed *fog* from the female germline at high levels (*nanos*::VP16-Gal4; pUASP-*fog*), which has previously been shown to overactivate the Fog pathway (Dawes-Hoang *et al.* 2005). This resulted in a severely defective cuticle phenotype, with only small amounts of recognizable cuticle remaining (Figure 4F). Remarkably however, loss of *tsl* function strongly suppressed the effects of ectopic Fog, resulting in cuticles more closely resembling the tsl^{Δ} phenotype (Figure 4G). However, we note that despite being null for *tsl*, many of these embryos no longer had ventral cuticle holes, possibly due to a partial rescue of tsl^{Δ} by residual Fog activity. Together, these data strongly suggest that Fog activity and the Rho1 pathway depend upon the maternal action of Tsl for morphogenesis.

Discussion

The apical constriction of cells underlies the critical ability of animal tissues to fold and change shape during development.

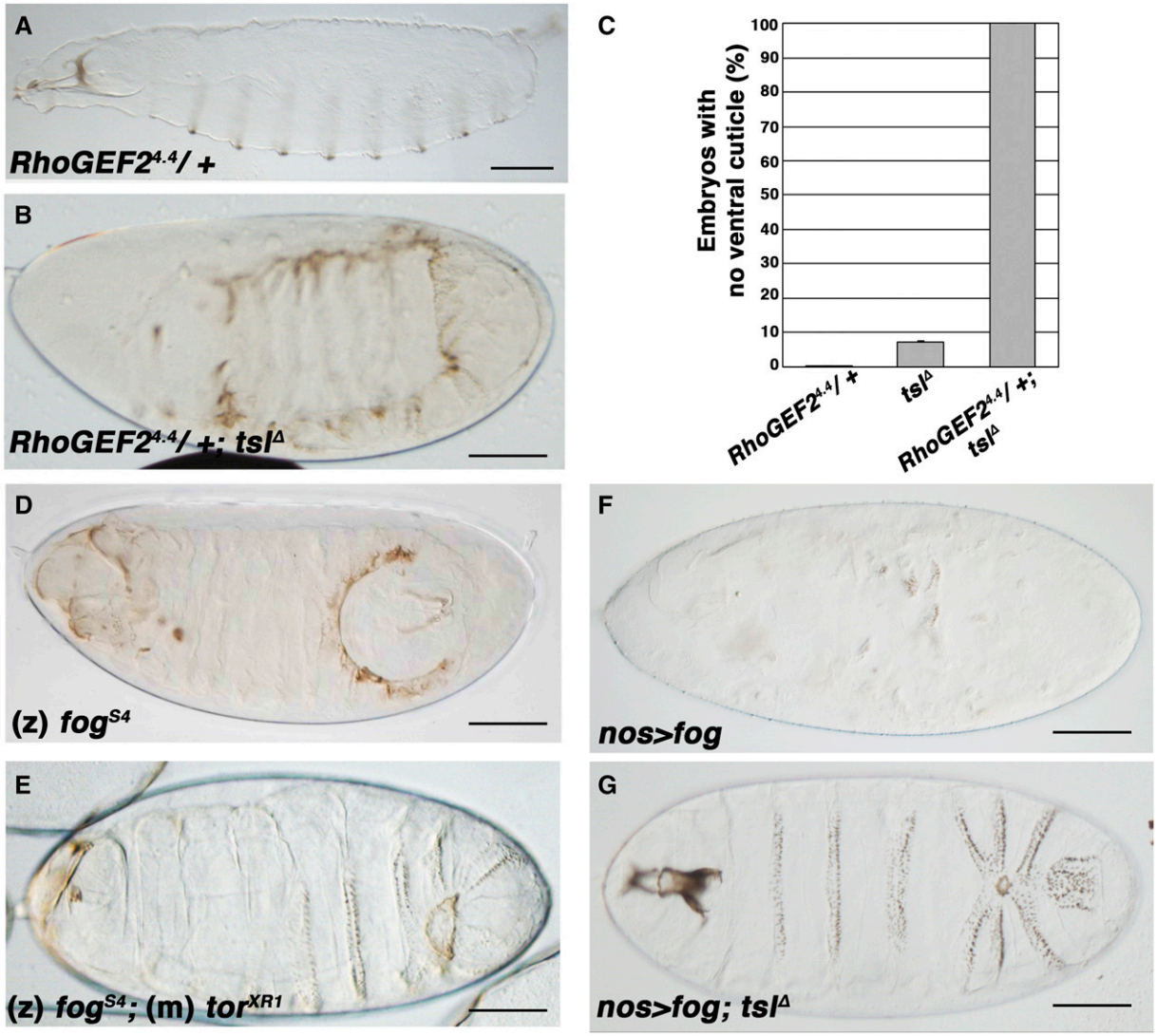

Figure 4 *tsl* interacts with *RhoGEF2* and *fog* in ventral morphogenesis. (A) Progeny from *RhoGEF2*$^{4.4}$ heterozygote females display a wild-type cuticle pattern. (B) Progeny from females heterozygous for *RhoGEF2*$^{4.4}$ and lacking *tsl* (*tsl*$^{\Delta}$) display a severe loss of ventral cuticle. (C) A striking increase in the proportion of embryos lacking ventral cuticles is observed when *RhoGEF2* dosage is reduced in a *tsl*$^{\Delta}$ background compared to *tsl*$^{\Delta}$ alone (*tsl*$^{\Delta}$ = 7.3% *vs.* *RhoGEF24.4*/+; *tsl*$^{\Delta}$ = 100%). Means are plotted and error bars represent one SE calculated from at least three cuticle preparations (> 100 cuticles scored for each). (D) Posterior–ventral holes are observed in cuticles of *fog*^{s4} embryos. (E) *fog*^{s4};*tor*^{XR1} double-mutant embryos have a cuticle phenotype that closely resembles that of *tsl*$^{\Delta}$. (F) Embryos from females expressing *fog* ubiquitously from the maternal germline (nos>) are severely compromised in their ability to produce ventral cuticle. (G) The cuticle phenotype of embryos that express *fog* in the absence of *tsl* closely resembles the *tsl*$^{\Delta}$ phenotype. Maternal genotypes are shown unless otherwise indicated (m, maternal; z, zygotic). Anteriors are to the left, ventral is down. Bar, 100 μm.

While the intracellular mechanisms that govern this process, including the involvement of the highly conserved Rho1 pathway, are quite well-characterized, relatively little is known about the extracellular signals that coordinate this process. Here, we make the unexpected finding that Tsl plays a second maternal role as a key extracellular component of the Fog/Rho1 pathway.

Extensive characterization of the role of Fog in the ventral furrow has demonstrated its importance in the coordination of cellular apical constriction in the cells of the ventral domain (Costa *et al.* 1994; Oda and Tsukita 2001; Dawes-Hoang *et al.* 2005; Fuse *et al.* 2013; Manning *et al.* 2013). Consistent with the phenotype of Fog mutants, we find that loss of maternal Tsl leads to irregular and uncoordinated ventral cell apical constrictions, incomplete furrow formation, and resultant ventral cuticle holes. Furthermore, we find that the activity of ectopic ubiquitous Fog delivered through the maternal germline is highly dependent on Tsl, suggesting that Tsl serves to regulate ventral Fog activity.

tsl has been studied for many years in its terminal patterning role, so it is somewhat surprising that the ventral cuticle defects described here have not been previously reported. This may be because most terminal patterning studies have utilized hypomorphic alleles of *tsl*. Here, we found that the ventral cuticle defects are only observed in embryos laid by homozygotes of the null allele, or when the null allele is

placed *in trans* with those hypomorphic alleles of *tsl* that have been reported to be stronger with respect to terminal patterning (*tsl*^{4} and *tsl*^{5}; Savant-Bhonsale and Montell 1993). We also made the surprising finding that the ventral morphogenesis defects we observed in *tsl* mutants can be rescued by expressing *tsl* in the same polar ovarian cells required for its function in terminal patterning. These data accordingly suggest that the same population of Tsl molecules is involved in both roles.

How might polar localized Tsl influence ventral Fog activity? Recent data on the role of Tsl in terminal patterning suggest that it mediates the extracellular accumulation of the ligand for the Tor receptor, Trk (Johnson *et al.* 2015). Thus, one possibility is that Tsl acts to directly mediate the secretion or activity of Fog. However, this idea seems unlikely as the overlap between the ventral cells that produce Fog and polar localized Tsl would be small or nonexistent. Furthermore, mosaic analyses by Costa *et al.* (1994) estimated that Fog could induce apical constriction only two to three cells away from its cell of origin. In addition, since immunostaining experiments by Mineo *et al.* (2015) have shown that Tsl remains localized to the embryo termini plasma membrane, we therefore reason that it is improbable that Tsl could directly influence Fog produced at the center of the embryo. Accordingly, an alternative idea is that Tsl is responsible for the extracellular accumulation of a hitherto unidentified molecule that can diffuse to the ventral region and control local Fog activity. A mechanism such as this might aid in coordinating the timing of apical constriction and subsequent furrow formation by controlling extracellular Fog activity uniformly across the cells of the ventral domain.

Is *tsl* also required for other *fog*-dependent morphogenetic events? Previous work has implicated *fog* in several other developmental roles, including morphogenesis of the larval wing disc (Nikolaidou and Barrett 2004; Manning *et al.* 2013), salivary gland formation during midembryogenesis (Lammel and Saumweber 2000), and invagination of the posterior midgut (the second major morphogenetic movement during gastrulation; Costa *et al.* 1994). While it remains possible that maternal *tsl* contributes to salivary gland morphogenesis and posterior midgut invagination, the dependence of these processes upon Tor signaling through the activities of target genes *tailless* and *forkhead* (Weigel *et al.* 1989; Costa *et al.* 1994; Wu and Lengyel 1998) precludes our ability to determine whether this is the case. In addition, since *tsl*$^{\Delta}$ adults have no discernable wing defects, we reason that Tsl is unlikely to play a role in wing morphogenesis. Determining if Tsl is required in other *fog*-mediated processes is thus challenging and will require sophisticated further studies.

The finding that maternal Tsl functions in two distinct processes during early *Drosophila* embryogenesis further raises the question as to whether Tsl was coopted from one role to the other during the course of evolution. Interestingly, bioinformatic studies of patterning pathway components in *Drosophila* and other insects have revealed that the function of Tsl in terminal patterning is likely a relatively recent adaptation (Duncan *et al.* 2013). For example, the honeybee uses an alternative terminal patterning system to Tor signaling, as its genome lacks *tor*- and *trk*-encoding sequences (Duncan *et al.* 2013). Further, in the honeybee, *tsl* is expressed ubiquitously in ovarian tissue, suggesting that its maternal function is not spatially restricted as it is in *Drosophila*. In addition, a recent study used RNA interference to knockdown *tsl* transcripts in the milkweed bug (*Oncopeltus fasciatus*), which like the honeybee also lacks the canonical terminal patterning pathway (Weisbrod *et al.* 2013). Intriguingly, rather than yielding terminal patterning defects, embryonic invagination defects were observed, indicating that Tsl may also function in morphogenesis in this insect. Together, these studies infer that the ancestral role of maternal Tsl in insects may have been in morphogenesis rather than terminal patterning. Furthermore, they raise the possibility that the localizing activity of Tsl, which has been its defining feature in terminal patterning, may instead represent a novel exploitation of its molecular function.

Tsl is a member of the pore forming perforin-like protein superfamily (Ponting 1999; Rosado *et al.* 2007). However, in contrast to most perforin-like proteins, which function as immune effectors or virulence factors, Tsl is instead critical for cell signaling during insect development. While we are yet to determine whether Tsl functions via pore formation or indeed via another mechanism of action, it is clear that its activity is crucial for several processes during fly development (Stevens *et al.* 1990; Grillo *et al.* 2012; Johnson *et al.* 2013; Forbes-Beadle *et al.* 2016). However, to date our ability to identify the commonalities and differences between these roles has been hampered by our lack of knowledge of the genetic pathways in which Tsl operates.

The data presented here suggest that, remarkably, Tsl serves to control two molecularly distinct signaling pathways in the context of the same early embryonic extracellular space. Tor is a receptor tyrosine kinase that signals through the Ras and mitogen-activated protein kinase cassette to influence cellular transcription (Sprenger *et al.* 1989), whereas Mist is a G-protein-coupled receptor that modulates the actomyosin cytoskeleton via G-protein signaling and the Rho1 GTPase (Manning *et al.* 2013). Therefore, we reason that the apparent lack of similarities between the Trk/Tor and Fog/Mist pathways, together with the influence of Tsl on extracellular Trk accumulation, is more in keeping with a function for Tsl in the regulation of either trafficking or secretion. Indeed, it will be interesting to learn how the active Mist ligand is generated and whether a Tsl-regulated event common to both ventral morphogenesis and terminal patterning is involved. Such information will undoubtedly provide valuable insights for our understanding of both the cellular coordination of tissue folding and of how perforin-like proteins function during development.

Acknowledgments

We thank Lauren Forbes Beadle and the Australian *Drosophila* Biomedical Research Facility (OzDros) for technical support, and also acknowledge support from Monash Micro Imaging and the Australian Research Council (ARC) Centre of Excellence in Advanced Molecular Imaging. We thank the Bloomington *Drosophila* Stock Centre for providing fly stocks, and the Developmental Studies Hybridoma Bank and Michael Murray for antibodies. We further thank Eric Wieschaus for discussions and Michelle Henstridge for critical reading of the manuscript. T.K.J. is an ARC Discovery Early Career Researcher Award Fellow. J.C.W. is a National Health and Medical Research Council of Australia Senior Principal Research Fellow.

Author contributions: T.K.J., J.C.W., and C.G.W. conceived the experiments and interpreted the data, co-led the work, and wrote the paper; T.K.J. and K.A.M. performed experiments.

Literature Cited

Barrett, K., M. Leptin, and J. Settleman, 1997 The Rho GTPase and a putative RhoGEF mediate a signaling pathway for the cell shape changes in *Drosophila* gastrulation. Cell 91: 905–915.

Bischof, J., R. K. Maeda, M. Hediger, F. Karch, and K. Basler, 2007 An optimized transgenesis system for *Drosophila* using germ-line-specific phiC31 integrases. Proc. Natl. Acad. Sci. USA 104: 3312–3317.

Casanova, J., and G. Struhl, 1989 Localized surface activity of torso, a receptor tyrosine kinase, specifies terminal body pattern in *Drosophila*. Genes Dev. 3: 2025–2038.

Costa, M., E. T. Wilson, and E. Wieschaus, 1994 A putative cell signal encoded by the folded gastrulation gene coordinates cell shape changes during *Drosophila* gastrulation. Cell 76: 1075–1089.

Cox, R. T., C. Kirkpatrick, and M. Peifer, 1996 Armadillo is required for adherens junction assembly, cell polarity, and morphogenesis during *Drosophila* embryogenesis. J. Cell Biol. 134: 133–148.

Dawes-Hoang, R. E., K. M. Parmar, A. E. Christiansen, C. B. Phelps, A. H. Brand *et al.*, 2005 folded gastrulation, cell shape change and the control of myosin localization. Development 132: 4165–4178.

Duncan, E. J., M. A. Benton, and P. K. Dearden, 2013 Canonical terminal patterning is an evolutionary novelty. Dev. Biol. 377: 245–261.

Forbes-Beadle, L., T. Crossman, T. K. Johnson, R. Burke, C. G. Warr *et al.*, 2016 Development of the cellular immune system of *Drosophila* requires the membrane attack complex/perforin-like protein Torso-like. Genetics 204: 675–681.

Fuse, N., F. Yu, and S. Hirose, 2013 Gprk2 adjusts Fog signaling to organize cell movements in *Drosophila* gastrulation. Development 140: 4246–4255.

Grillo, M., M. Furriols, C. de Miguel, X. Franch-Marro, and J. Casanova, 2012 Conserved and divergent elements in Torso RTK activation in *Drosophila* development. Sci. Rep. 2: 762.

Hacker, U., and N. Perrimon, 1998 DRhoGEF2 encodes a member of the Dbl family of oncogenes and controls cell shape changes during gastrulation in *Drosophila*. Genes Dev. 12: 274–284.

Hortsch, M., N. H. Patel, A. J. Bieber, Z. R. Traquina, and C. S. Goodman, 1990 *Drosophila* neurotactin, a surface glycoprotein with homology to serine esterases, is dynamically expressed during embryogenesis. Development 110: 1327–1340.

Ip, Y. T., and T. Gridley, 2002 Cell movements during gastrulation: snail dependent and independent pathways. Curr. Opin. Genet. Dev. 12: 423–429.

Jimenez, G., A. Gonzalez-Reyes, and J. Casanova, 2002 Cell surface proteins Nasrat and Polehole stabilize the Torso-like extracellular determinant in *Drosophila* oogenesis. Genes Dev. 16: 913–918.

Johnson, T. K., T. Crossman, K. A. Foote, M. A. Henstridge, M. J. Saligari *et al.*, 2013 Torso-like functions independently of Torso to regulate *Drosophila* growth and developmental timing. Proc. Natl. Acad. Sci. USA 110: 14688–14692.

Johnson, T. K., M. A. Henstridge, A. Herr, K. A. Moore, J. C. Whisstock *et al.*, 2015 Torso-like mediates extracellular accumulation of Furin-cleaved Trunk to pattern the *Drosophila* embryo termini. Nat. Commun. 6: 8759.

Kam, Z., J. S. Minden, D. A. Agard, J. W. Sedat, and M. Leptin, 1991 *Drosophila* gastrulation: analysis of cell shape changes in living embryos by three-dimensional fluorescence microscopy. Development 112: 365–370.

Knust, E., and H. J. Muller, 1998 *Drosophila* morphogenesis: orchestrating cell rearrangements. Curr. Biol. 8: R853–R855.

Kolsch, V., T. Seher, G. J. Fernandez-Ballester, L. Serrano, and M. Leptin, 2007 Control of *Drosophila* gastrulation by apical localization of adherens junctions and RhoGEF2. Science 315: 384–386.

Lammel, U., and H. Saumweber, 2000 X-linked loci of *Drosophila melanogaster* causing defects in the morphology of the embryonic salivary glands. Dev. Genes Evol. 210: 525–535.

Lecuit, T., and P. F. Lenne, 2007 Cell surface mechanics and the control of cell shape, tissue patterns and morphogenesis. Nat. Rev. Mol. Cell Biol. 8: 633–644.

Leptin, M., 1995 *Drosophila* gastrulation: from pattern formation to morphogenesis. Annu. Rev. Cell Dev. Biol. 11: 189–212.

Leptin, M., and B. Grunewald, 1990 Cell shape changes during gastrulation in *Drosophila*. Development 110: 73–84.

Leptin, M., J. Casal, B. Grunewald, and R. Reuter, 1992 Mechanisms of early *Drosophila* mesoderm formation. Dev. Suppl. 1992: 23–31.

Manning, A. J., K. A. Peters, M. Peifer, and S. L. Rogers, 2013 Regulation of epithelial morphogenesis by the G protein-coupled receptor mist and its ligand fog. Sci. Signal. 6: ra98.

Martin, A. C., M. Gelbart, R. Fernandez-Gonzalez, M. Kaschube, and E. F. Wieschaus, 2010 Integration of contractile forces during tissue invagination. J. Cell Biol. 188: 735–749.

Martin, J. R., A. Raibaud, and R. Ollo, 1994 Terminal pattern elements in *Drosophila* embryo induced by the torso-like protein. Nature 367: 741–745.

Mineo, A., M. Furriols, and J. Casanova, 2015 Accumulation of the *Drosophila* Torso-like protein at the blastoderm plasma membrane suggests that it translocates from the eggshell. Development 142: 1299–1304.

Morize, P., A. E. Christiansen, M. Costa, S. Parks, and E. Wieschaus, 1998 Hyperactivation of the folded gastrulation pathway induces specific cell shape changes. Development 125: 589–597.

Nikolaidou, K. K., and K. Barrett, 2004 A Rho GTPase signaling pathway is used reiteratively in epithelial folding and potentially selects the outcome of Rho activation. Curr. Biol. 14: 1822–1826.

Oda, H., and S. Tsukita, 2001 Real-time imaging of cell-cell adherens junctions reveals that *Drosophila* mesoderm invagination begins with two phases of apical constriction of cells. J. Cell Sci. 114: 493–501.

Ponting, C. P., 1999 Chlamydial homologues of the MACPF (MAC/perforin) domain. Curr. Biol. 9: R911–R913.

Ray, R. P., K. Arora, C. Nusslein-Volhard, and W. M. Gelbart, 1991 The control of cell fate along the dorsal-ventral axis of the *Drosophila* embryo. Development 113: 35–54.

Rorth, P., 1998 Gal4 in the *Drosophila* female germline. Mech. Dev. 78: 113–118.

Rorth, P., K. Szabo, A. Bailey, T. Laverty, J. Rehm *et al.*, 1998 Systematic gain-of-function genetics in *Drosophila*. Development 125: 1049–1057.

Rosado, C. J., A. M. Buckle, R. H. Law, R. E. Butcher, W. T. Kan *et al.*, 2007 A common fold mediates vertebrate defense and bacterial attack. Science 317: 1548–1551.

Rubin, G. M., and A. C. Spradling, 1982 Genetic transformation of *Drosophila* with transposable element vectors. Science 218: 348–353.

Rubin, G. M., L. Hong, P. Brokstein, M. Evans-Holm, E. Frise *et al.*, 2000 A *Drosophila* complementary DNA resource. Science 287: 2222–2224.

Savant-Bhonsale, S., and D. J. Montell, 1993 torso-like encodes the localized determinant of *Drosophila* terminal pattern formation. Genes Dev. 7: 2548–2555.

Sawyer, J. M., J. R. Harrell, G. Shemer, J. Sullivan-Brown, M. Roh-Johnson *et al.*, 2010 Apical constriction: a cell shape change that can drive morphogenesis. Dev. Biol. 341: 5–19.

Sprenger, F., and C. Nusslein-Volhard, 1992 Torso receptor activity is regulated by a diffusible ligand produced at the extracellular terminal regions of the *Drosophila* egg. Cell 71: 987–1001.

Sprenger, F., L. M. Stevens, and C. Nusslein-Volhard, 1989 The *Drosophila* gene torso encodes a putative receptor tyrosine kinase. Nature 338: 478–483.

Stevens, L. M., H. G. Frohnhofer, M. Klingler, and C. Nusslein-Volhard, 1990 Localized requirement for torso-like expression in follicle cells for development of terminal anlagen of the *Drosophila* embryo. Nature 346: 660–663.

Sweeton, D., S. Parks, M. Costa, and E. Wieschaus, 1991 Gastrulation in *Drosophila*: the formation of the ventral furrow and posterior midgut invaginations. Development 112: 775–789.

Tomancak, P., A. Beaton, R. Weiszmann, E. Kwan, S. Shu *et al.*, 2002 Systematic determination of patterns of gene expression during Drosophila embryogenesis. Genome Biol. 3: RESEARCH0088.

Weigel, D., G. Jurgens, F. Kuttner, E. Seifert, and H. Jackle, 1989 The homeotic gene fork head encodes a nuclear protein and is expressed in the terminal regions of the *Drosophila* embryo. Cell 57: 645–658.

Weisbrod, A., M. Cohen, and A. D. Chipman, 2013 Evolution of the insect terminal patterning system–insights from the milkweed bug, *Oncopeltus fasciatus*. Dev. Biol. 380: 125–131.

Wieschaus, E., and C. Nüsslein-Volhard, 1986 Looking at embryos, pp. 199–227 in *Drosophila: A Practical Approach*, edited by D. B. Roberts. IRL Press, Oxford.

Wieschaus, E., C. Nüsslein-Volhard, and G. Jürgens, 1984 Mutations affecting the pattern of the larval cuticle in *Drosophila melanogaster*. Rouxs Arch. Dev. Biol. 193: 296–307.

Wu, L. H., and J. A. Lengyel, 1998 Role of caudal in hindgut specification and gastrulation suggests homology between *Drosophila* amnioproctodeal invagination and vertebrate blastopore. Development 125: 2433–2442.

Zusman, S. B., and E. F. Wieschaus, 1985 Requirements for zygotic gene activity during gastrulation in *Drosophila melanogaster*. Dev. Biol. 111: 359–371.

Communicating editor: R. J. Duronio